HHS Public Access

Author manuscript

J Neurosci Res. Author manuscript; available in PMC 2020 February 11.

Published in final edited form as:

J Neurosci Res. 2019 February ; 97(2): 137–148. doi:10.1002/jnr.24335.

Blood-Brain barrier disruption and angiogenesis in a rat model for neurocysticercosis

Rogger P. Carmen-Orozco[1], **Danitza G. Dávila**[1], **Yudith Cauna**[1], **Edson G. Bernal**[1], **Leandra Bitterfeld**[2], **Graham L. Sutherland**[2], **Nancy Chile**[1], **Rensson H. Céliz**[1], **María C. Ferrufino-Schmidt**[1], **Cesar Gavídia**[3], **Charles R. Sterling**[4], **Héctor H. García**[1,5], **Robert H. Gilman**[1,2,6], **Manuela R. Verástegui**[1] **Cysticercosis Working Group in Peru**

[1.]Infectious Diseases Laboratory Research-LID, Faculty of Science and Philosophy, Alberto Cazorla Talleri, Universidad Peruana Cayetano Heredia, Lima, Perú. [2.]The Department of International Health, Bloomberg School of Hygiene and Public Health, The Johns Hopkins University, Baltimore, Maryland, USA. [3.]School of Veterinary Medicine, Universidad Nacional Mayor de San Marcos, Lima, Perú. [4.]School of Animal and Comparative Biomedical Sciences, University of Arizona, Tucson, Arizona, USA. [5.]Cysticercosis Unit, Instituto de Nacional Ciencias Neurológicas, Lima, Perú. [6.]Asociación Benéfica PRISMA, Lima, Perú.

Abstract

Neurocysticercosis (NCC) is a helminth infection affecting the central nervous system caused by the larval stage (cysticercus) of *Taenia solium.* Since vascular alteration and blood-brain-barrier (BBB) disruption contribute to NCC pathology, it is postulated that angiogenesis could contribute to the pathology of this disease. This study used a rat model for NCC and evaluated the expression of two angiogenic factors called vascular endothelial growth factor (VEGF-A) and fibroblast growth factor (FGF2). Also, two markers for BBB disruption, the endothelial barrier antigen and immunoglobulin G, were evaluated using immunohistochemical and immunofluorescence techniques. Brain vasculature changes, BBB disruption, and overexpression of angiogenesis markers surrounding viable cysts were observed. Both VEGF-A and FGF2 were overexpressed in the tissue surrounding the cysticerci, and VEGF-A was overexpressed in astrocytes. Vessels showed decreased immunoreactivity to endothelial barrier antigen marker and an extensive staining for IgG was found in the tissues surrounding the cysts. Additionally, an endothelial cell tube formation assay using human umbilical vein endothelial cells showed that excretory and secretory antigens of *T. solium* cysticerci induce the formation of these tubes. This *in vitro* model supports the hypothesis that angiogenesis in NCC might be caused by the parasite itself, as opposed to the host inflammatory responses alone.

Corresponding author. Tel.: +051-483 2942., address: manuela.verastegui@upch.pe (M. Verastegui).

AUTHOR CONTRIBUTIONS

All authors had full access to all the data in the study and take responsibility for the integrity of the data and the accuracy of the data analysis. *Conceptualization*, RP. C. and MR. V.; *Methodology*, RP. C., DG.D., N.C. and MR. V.; *Investigation*, RP. C., DG. D., Y.C., EG. B., GL. S., RH. C and MC. F-S.; *Formal Analysis*, RP. C; *Resources*: MR. V., HH. G. and RH. G.; *Writing – Original Draft*, RP. C.; *Writing – Review & Editing*, RP. C., L. B., GL. S., C. G., CR. S., HH. G., RH. G. and MR. V.; *Visualization*, RP. C.; *Supervision*, RH. G. and MR. V.; Project Administration, MR. V.; *Funding Acquisition*, RH. G., HH. G. and MR.V. All authors reviewed the manuscript.

The authors have no conflict of interest to declare

Conclusion ––—Brain vasculature changes, BBB disruption, and overexpression of angiogenesis markers surrounding viable cysts were observed. This study also demonstrates that cysticerci excretory-secretory processes alone can stimulate angiogenesis.

Keywords

T. solium; neurocysticercosis; BBB disruption; angiogenesis; VEGF-A

INTRODUCTION

Neurocysticercosis (NCC) is the most common helminth infection affecting the central nervous system (CNS)(de Aluja, González, Rodríguez Carbajal, & Flisser, 1989; Escobar, Aruffo, Cruz-Sánchez, & Cervos-Navarro, 1985). While pigs are the natural host of *Taenia solium* cysticerci, humans may be accidentally infected following ingestion of *T. solium* eggs, which subsequently develop into cysticerci (Escobar et al., 1985; Nash & Garcia, 2011). Symptomatic NCC patients present with epilepsy as the main clinical manifestation. In developing countries where *T. solium* is endemic and pigs are raised freely (Garcia & Del Brutto, 2005), 29% of adult cases of epilepsy are due to NCC (Ndimubanzi et al., 2010).

The study of biopsies in NCC patients and the use of animal models have established that the pathology varies according to the number, location, and viability of the cysticerci (Chandy et al., 1989; Guerra-Giraldez et al., 2013; Marzal et al., 2014). The use of imaging techniques such as magnetic resonance imaging (MRI) and computerized tomography (CT) have allowed for the identification of inflammatory reactions and the grade of cysticerci degeneration (Oscar H Del Brutto, 2012; Shetty, Avabratha, & Rai, 2014). However, such techniques, do not provide information about either physiological or molecular changes in the disease. Pathological characteristics of NCC in humans and pigs include the presence of inflammatory cells, fibrosis, gliosis, and blood-brain-barrier (BBB) disruption surrounding the parasite (J. I. Alvarez, Londoño, et al., 2002; Marzal et al., 2014; Restrepo et al., 2001; Sikasunge, Johansen, Phiri, Willingham, & Leifsson, 2009).

Angiogenesis and disruption of the BBB could contribute to the pathogenesis of NCC in humans (Restrepo et al., 2001). Vascular alteration, occlusion, and thickness of vessels have been reported in postmortem samples of patients (O. H. Del Brutto, 1992), while BBB disruption in pigs with NCC has also been observed (Marzal et al., 2014). Studies have shown that BBB disruption and extravasation of serum proteins into the cerebral parenchyma promotes epileptogenesis (Bar-Klein et al., 2014; Ivens et al., 2007), a major symptom of NCC. Furthermore, vascular alterations, angiogenesis, and BBB disruption are present in various chronic disorders of the CNS, such as stroke, ischemia, Parkinson's disease, and Alzheimer's disease (Carmeliet, 2003). It is interesting to note that, according to one study, the degree of such cerebrovascular changes present in CNS disorders is correlated with prognosis. That is, the greater the cerebrovascular alteration, the worse the prognosis (Renú et al., 2015). How these changes contribute to NCC pathology and prognosis, specifically, is still unknown.

Animal models, including rodents, pigs, and monkeys have been developed to study the pathology of NCC (Arora et al., 2017). Although rodent models are the most commonly

used, none have been successful in infecting rodent brains with *T. solium* cysticerci (Jorge I. Alvarez, Mishra, Gundra, Mishra, & Teale, 2010; Matos-Silva et al., 2012). In this study, however, we used a recently published rat model for NCC (rNCC) in which rats were successfully infected through intracranial inoculation of activated *T. solium* oncospheres (M. R. Verastegui et al., 2015). The cysts that develop using this model have the same morphological characteristics and similar basic pathological responses, i.e. presence of fibrotic tissue encapsulating the cyst, gliosis and cellular infiltrates, as found in human NCC. Thus, we used this model to explore angiogenic and BBB disruption in NCC infection. This study investigated the vascular pathology of rNCC and *in vitro* responses to the cyst by evaluating the expression of two angiogenic factors (VEGF-A and FGF2). BBB disruption was studied by evaluating the presence of IgG in parenchyma and the expression of endothelial barrier antigen (EBA), fibrinogen, and Evans blue extravasation. Finally, the study used an *in vitro* model with human umbilical vein endothelial cells (HUVEC) to determine if the excretory-secretory products of the *T. solium* cyst could induce angiogenesis.

MATERIALS AND METHODS

The Universidad Peruana Cayetano Heredia guidelines for care and use of animals were used to conduct the experiments (IACUC number 64637).

T. solium egg processing.

Procedures were performed according to Verástegui et al (M. Verastegui et al., 2007). Briefly, *T. solium* eggs were washed 3 times with distilled water and centrifuged at 2500 rpm RT for 5 minutes. To obtain oncospheres, the pellet was resuspended in 0.75% sodium hypochlorite solution and washed 3 times using RPMI medium. The oncospheres were then activated by incubation in artificial intestinal fluid (AIF) for 45 minutes at 37°C, washed 3 times in RPMI medium, and counted in a Neubauer chamber.

Animal infection.

Holtzman rats, aged 12 to 15 days (P12-P15), were used as a model for NCC. Eighteen rats (11 males, 7 females) were injected intracranially with 140 activated oncospheres resuspended in 50ul of saline solution. Nine control rats (4 female, 5 males) received only saline, and their brains were used as control regions for all the comparisons. The intracranial injection was performed using tuberculin syringes and a 25-gauge needle, inserted 2 mm deep in the anterior fontanelle (bregma). This method circumvented parenchymal damage (M. R. Verastegui et al., 2015). Animals were anesthetized before the injection using Ketamine (80 mg/kg) and Xylazine (5 mg/kg); the absence of pedal reflex was checked to determine proper anesthesia. Rats were fed ad libitum in 12 hours of a light and dark cycle at the UPCH animal care facility. Area of intracranial injection was monitored daily for one week by visual inspection; no changes were observed.

Tissue processing.

Female (280–320g) and male rats (400–450g) were euthanized and sacrificed after six months of infection using an overdose of Ketamine (150 mg/kg) and Xylazine (20 mg/kg).

The rats were perfused with phosphate buffered saline (PBS) at a pH of 7.2, followed by a 4% paraformaldehyde (PFA) solution. Brains were then post-fixed overnight in PBS/PFA solution. Three groups of animals were used. The first group (18 animals mentioned) was used to obtain paraffin sections. Brains were processed according to standard histologic techniques, and 4um thick slices were cut and stained using Masson's trichrome technique. The second group (4 animals, 2 male, and 2 female rats) was used for cryostat sections. After post-fixation, brains were washed in distilled water, immersed in 30% sucrose, embedded in optimal cutting temperature (OCT), and slices of 30 μm were obtained at −20°C. In order to detect protein extravasation of the brain parenchyma, a third group of 5 infected female rats were injected i.p. with 4mg/kg of evans blue solution diluted in sterile PBS. After 12 hours, animals were anesthetized (150 mg/kg Ketamine and 20mg/kg Xylazine) and perfused with PBS solution and 4% PFA/PBS solution. Brains were extracted and embedded in OCT, slices of 30μm were obtained, mounted with ProLong® Gold Antifade Mountant with DAPI and observed under ZEISS LSM 880 Airyscan confocal microscope.

Immunohistochemistry (IHC).

The paraffin sections were heated in an oven at 56°C, immersed in xylene, and rehydrated in a decreasing battery of alcohols. The sections were then unmasked using a different method for each marker employed (Table S1). Next, the sections were washed with PBS and endogenous peroxidase activity was blocked by the addition of 3% hydrogen peroxide for 30 minutes. After incubation for 1 hour in protein blocking solution, the slices were incubated with their respective primary antibody (Anti-VEGF-A, Anti-FGF2, Anti-EBA, Rat Anti-IgG). The slices were then washed and incubated with their respective secondary antibody. In cases where biotin-labeled secondary antibody was employed, the slices were washed and incubated in streptavidin HRP-labeled solution. Sections were revealed using diaminobenzidine (DAB, Dako) solution, counterstained with hematoxylin, and mounted in Entellan solution (MERCK).

Immunofluorescence.

Thirty μm cryostat sections were used for confocal imaging (four infected and two uninfected brains). Sections were placed in 12-well microplates containing PBS. Sections were permeabilized in 1% Triton X-100 PBS overnight, then washed with PBS. Each primary antibody was added (rabbit anti-VEGF-A or mouse anti-FGF2), incubated for 2 days, washed, and covered with their respective secondary antibody for 3 hours (Donkey anti-rabbit IgG Alexa Fluor® 488 labeled, or donkey anti-mouse IgG Alexa Fluor® 488 labeled). A second primary antibody for glial detection was added (mouse anti-GFAP, rabbit anti GFAP, or goat anti-Iba-1), incubated for 2 days at 4°C, washed, and incubated with their respective secondary antibody for 3 hours (Donkey anti-mouse IgG Alexa Fluor® 594 labeled, donkey anti-rabbit IgG Alexa Fluor® 594 labeled, or donkey anti-goat IgG Alexa Fluor® 594 labeled). Finally, sections were mounted using ProLong® Gold Antifade Mountant with DAPI.

Image acquisition and tissue analysis.

IHC imaging was performed using an Axiocam ERc5 camera coupled to a Zeiss Axio Lab.A1 microscope. 6 images of the tissue closely surrounding the cyst were acquired. Cysticerci were classified according to Cangalaya et al (Cangalaya et al., 2015) and included parenchymal, corticomeningeal, and ventricular cysts. Meningeal cysticerci were not considered because they frequently detach during tissue processing. For control regions, images of the entire cortex from non-infected animals were used for comparison with parenchymal and corticomeningeal cysts, since most cysticerci were located in the cortex. Additionally, 6 images from areas surrounding ventricles were taken to analyze lateral ventricular cysts. Their respective control regions were obtained from the tissue surrounding the lateral ventricles of non-infected rats. Images were processed using ImageJ v1.21 and a deconvolution method (Ruifrok & Johnston, 2001) was applied before measurement of the immunoreactive area (proportion between the number of pixels stained over the total number of pixels in each image) for each marker (VEGF-A (400x), FGF2 (400x), and IgG (100x)). The average of the 6 values for the immunoreactive area for each cyst or each control was used for comparison. Finally, 10 images surrounding the cysts or control region were taken at 400x total magnification for EBA slides. EBA non-immunoreactive vessel numbers were counted manually using ImageJ v1.21. Non-immunoreactive vessels were identified as endothelial cells having elongated nuclei and cytoplasm without DAB reaction. Immunofluorescent images obtained from cryosections were acquired using a ZEISS LSM 880 Airyscan confocal microscope. Images were organized using Adobe Photoshop CS6 software.

In vitro model of angiogenesis.

Antigen preparation.—Excretory-secretory (E/S) antigens were collected from a culture of cysticerci. That is, viable cysticerci were obtained from muscles of an infected pig, placed in Vascular Cell Basal Medium for 24h, and the supernatant collected (E/S antigens). Protein concentration was measured using the Bradford assay and 25 μg/ml of E/S antigens were used in the tube formation assay. The antigen concentration used was based on previous results where E/S antigens induced cytokine production in human PBMC (unpublished data).

Tube formation assay.—Human Umbilical Vein Endothelial Cells (HUVEC, ATCC®PCS-100–010TM) were obtained from American Tissue Culture Collection (ATCC, Manassas, VA) and grown in 75-cm^2 tissue culture flasks (Corning) containing Vascular Cell Basal Medium (ATCC PCS-100–030) supplemented with the Growth Kit-BBE (ATCC PCS-100–040), as recommended by the manufacturer. HUVEC from passage 2 was used in this experiment. Then 500 μL of either basal medium, basal medium + E/S cysticerci products, or basal medium + VEGF (Endothelial Cell Growth Kit-VEGF) was placed into three different wells of a 24-well flat-bottomed plate coated with 289 μl of Matrigel per well (Corning® Basement Membrane Matrix). Cells were then trypsinized (trypsin/EDTA solution; ATCC PCS-999–003) and resuspended in 2×10^5 cell/ml in basal medium, basal medium with E/S, or complete medium. 500 μL of cell suspensions was slowly added to each well containing the appropriate medium and Matrigel (3 wells/condition) in order to yield a final concentration of 1×10^5 cells in 1 mL of medium in each well. After incubation

for an additional 18 hours, the medium was removed and the cells were fixed in 10% neutral buffered formalin. Cells were photographed at 40X total magnification and the number of branches were counted.

Statistical analysis.

All exploratory and statistical data analyses were performed using Stata v13. A Shapiro-Wilk test was used to evaluate the presence of normal distributions.. Since all of the groups were not normally distributed, the Mann-Whitney U test was used to compare between infected areas and their respective control areas.

RESULTS

Fibrosis and fibrotic vessels surround cysticercus in NCC model

Thirteen of the 18 inoculated rats (8 males and 5 females) developed cysts (72.2% rate of infection). All of the cysts showed intact teguments and angiogenic vessels and were considered viable. We had previously reported the presence of angiogenic vessels (22), but here were able to demonstrate three different types of vessel alterations. We observed dilated vessels without fibrosis, dilated vessels with perivascular fibrosis, and sclerotic vessels containing a dense layer of fibrotic tissue demonstrated by trichrome Masson staining (Fig 1). The cysts were classified according to their location. 11 cysts were considered parenchymal, 8 were considered corticomeningeal, and 8 were considered ventricular (Table S2). Vessel alterations were present in all cyst locations.

Angiogenic factors are overexpressed in the area surrounding the cyst and vary by location.

Non-infected tissue showed scarce staining for vascular endothelial growth factor A (VEGF-A) in the cortex and high immunoreactivity in subventricular areas. In infected brains, VEGF-A distribution was adjacent to fibrosis and showed a non-homogenous network pattern surrounding the cysts (Figure 2A, i-iv). The expression of VEGF-A, defined by the percentage of the area surrounding the cyst that was immunoreactive (Table S3), was greater in parenchymal and corticomeningeal cysts compared to control regions (Mann–Whitney U test $z=3.487$, $P<0.001$ and $z=3.240$, $P=0.001$, respectively, Figure 2A, v). Ventricular cysts tended to have increased VEGF-A expression when compared to their respective control tissue (Mann-Whitney U test $z=1.610$, $P=0.107$).

In the cerebral cortex of non-infected brains, nuclear staining of different types of neuronal and glial cells was observed during the evaluation of fibroblast growth factor 2 (FGF2, Fig. 2B, i-ii). In the ventricles, most ependymal cells showed an immune reaction for this marker. Infected brains showed high levels of FGF2 expression in the areas surrounding the parasite, including the area of fibrosis, and showed focal areas of high expression (Fig 2B, iii-iv). A statistically significant difference was only observed between parenchymal cysts and its control region when the area of immune reaction was compared (Mann-Whitney U test $z=2.939$, $P=0.003$; Fig 2B, v; Table S3). In addition, VEGF-A expression in parenchymal cysts of female rats [n=4] showed higher immunoreactivity compared to male rats [n=7]

(Mann-Whitney U test z=2.646, P=0.008). No differences were found when control brains or other cyst locations were compared for VEGF-A or FGF2.

GFAP and Iba-1 immunofluorescence reacted strongly in cells surrounding the parasite. Astrocytes positive to GFAP exhibited a gliotic network shape, and phagocytes positive to Iba-1 showed a widespread reaction close to the parasite. Double staining of VEGF-A and glial cells (GFAP or Iba-1 positives) in non-infected brain showed most cells colocalizing with GFAP, while a few colocalized to Iba-1. While infected brains showed a strong reaction between GFAP and VEGF-A, no colocalizing between Iba-1 and VEGF-A was detected, suggesting that most VEGF-A overexpression is produced by astrogliosis (Fig 3). No colocalization between FGF2 and Iba-1 was observed (data not shown).

BBB disruption in NCC model

In control brains, the immune reaction to IgG was absent in the cerebral parenchyma and minimal in the meninges (Fig 4A, i-ii). Moreover, the lumen of certain blood vessels showed immune reactivity to IgG without extravasation to the parenchyma. In the ventricles, the presence of IgG was found in the choroid plexus. However, n circumventricular regions, the IgG immunoreactivity was nearly absent. Infected brains had strong immunoreactivity surrounding the parasite, and a statistically significant difference was found in parenchymal, corticomeningeal, and ventricular cysts compared to their control regions (Mann-Whitney U test z=3.551, P<0.001, z=3.240, P=0.001, z=2.089, P=0.037, respectively; Fig 4A, iii-iv; Table S3). When comparing immune reactivity between the different cyst locations, parenchymal cysts had the strongest reaction. (Kruskal-Wallis test χ^2=11.247, P=0.004, Fig 4A, v). Additionally, there was a trend for IgG staining to increase when comparing infected female rats [n=4] to infected male rats [n=7] (Mann-Whitney U test z=1.701, P=0.089). No differences were found in other cyst location or control brains compared by sex.

Endothelial barrier antigen (EBA) staining demonstrated a strong reaction in the vascular endothelium of the cerebral cortex of control regions (Fig 4B, i-iii). Infected brains showed non-immunoreactive vessels, which strongly suggests disruption of the endothelial barrier. Vessels appear as cells with elongated nuclei and cytoplasm in areas surrounding cysts, so they were easily identifiable by their characteristic shape. (Fig 4B, iv-vii). Compared to controls, the number of non-immunoreactive vessels was significantly increased around parenchymal and corticomeningeal cysts, but not around ventricular cysts (Mann-Whitney U test z=3.178 P=0.002, z=3.362, P=0.001, and z=1.029, P=0.3036, respectively, Fig 4B, viii).

Evans blue extravasation was evaluated in five rats which resulted in only one rat with a stained corticomengineal cysticerci. The other four rats carried ventricular, parenchymal or corticomeningeal cysts (Fig. 5A). Evans blue extravasation to the parenchymal tissue was confirmed by confocal microscopy (Fig. 5A). Although fibrinogen staining was observed, it was likely present in the fibrotic tissue as part of the fibrosis which envelops the cyst. This was confirmed since most of the fibrinogen stained the same as the area detected with Masson’s trichrome staining (Fig. 5B). Fibrinogen was overexpressed in parenchymal and corticomeningeal cysts compared with non-infected animal cysts (Mann-Whitney U test z=3.317, P<0.001 and z=3.000, P=0.003, respectively). No differences were found when fibrinogen or EBA expression were compared by sex of the rats.

Extension and co-distribution of angiogenic markers and EBA

Our results showed that parenchymal and corticomeningeal cysts shared similar cellular responses for all the markers studied. To explore if there was a co-distribution in the extension of VEG-A, FGF2, and EBA around the parasite, a kernel density plot was constructed (Fig. 6). Interestingly, in parenchymal and corticomeningeal cysts, the kernel density plot demonstrated a co-distribution for all markers except for ventricular cysts (Fig. 6). In parenchymal and corticomeningeal cysts, VEGF-A, EBA, and FGF2 were denser at a distance of 100μm from the parasite. In contrast, FGF2 expression in ventricular cysts was densest at a distance of 50 μm from the parasite. Similar extension of VEGF-A and EBA was seen in all cyst locations, which could be found at distances of up to approximately 300μm from the parasite.

Cysticercus antigens induce tube formation in an *in vitro* model for angiogenesis

The Matrix based tube formation assay using HUVEC cells showed network development when incubated with basal media and either E/S cysticercus antigens or VEGF recombinant protein (Fig. 7). No network formation was observed when only basal media was added to the HUVEC culture (control). The number of branches was quantified and a statistically significant difference was found when comparing both E/S antigens and VEGF to the control (Mann-Whitney U test $z=-1.964$, $P<0.050$ for both cases). No statistically significant differences were found between E/S and VEGF (Fig. 7).

DISCUSSION

This study demonstrated brain vasculature changes, BBB disruption, and overexpression of angiogenesis markers surrounding viable cysts in intracranially inoculated rats. Changes in brain vasculature showed fibrosis and possible dysfunction in vessels surrounding the cysts. VEGF-A and FGF2, used for angiogenesis evaluation, were overexpressed in the tissue surrounding *T. solium* cysticerci, and their expression varied depending on the location of the parasite. Moreover, VEGF-A overexpression was associated with astrocytes, reflecting the possible importance of this cell's role in NCC pathology. In vitro assays also revealed that cysticercus antigens were able to induce angiogenesis. BBB evaluation showed that most of the cysticerci were associated with some degree of BBB alteration. Since only viable cysts were evaluated, this study indicates that BBB disruption begins even before a viable cyst starts degenerating, which potentially contributes to NCC pathogenesis.

VEGF-A was overexpressed in host tissue adjacent to parenchymal cysts and corticomeningeal cysts, whereas ventricular cysts had a non-significant increase in expression of VEGF-A. Such overexpression reflects major changes in cysts that are in close contact with the brain tissue. VEGF-A overexpression in astrocytes is associated with BBB disruption (Argaw et al., 2012; Argaw, Gurfein, Zhang, Zameer, & John, 2009; Argaw et al., 2006; Obermeier, Daneman, & Ransohoff, 2013; Sköld, Gertten, Sandbergnordqvist, Mathiesen, & Holmin, 2005). While our results showed VEGF-A overexpression in astroglia, this phenomenon was not seen in microglial cells, suggesting that a possible interaction exists between VEGF-A and BBB disruption in NCC pathology. VEGF-A is a mitogenic factor and *in vitro* studies have shown that it increases the proliferation and

mobility of astrocytes (Mani, Khaibullina, Krum, & Rosenstein, 2005). VEGF-A is also the principal protein which induces angiogenesis (Rosenstein, Mani, Silverman, & Krum, 1998) and its overexpression has been associated with many neuropathologies. However, the contribution of this protein to the pathology of NCC has not yet been studied. Studies in temporal lobe epilepsy have shown that angiogenesis is associated with BBB disruption (Rigau et al., 2007), so studying this association in NCC patients with epilepsy could be important.

FGF2 is a potent neurotrophic (Gómez-Pinilla, Lee, & Cotman, 1992) and angiogenic factor (Giavazzi et al., 2003). It is expressed in many cell types within the brain, including astrocytes, capillary endothelial cells, pericytes, and neurons (Araujo & Cotman, 1992; Baird & Walicke, 1989). In addition, FGF2 is a potent mitogenic factor and regulates proliferation of astrocytes (Gómez-Pinilla, Vu, & Cotman, 1995). Its overexpression found around the cysticerci could explain the marked presence of gliosis, fibrogenesis, and angiogenesis in NCC (Liu, Yang, & Chen, 1994). FGF2 overexpression has been reported in cerebral vessels in NCC patients with granulomas (J. I. Alvarez, Colegial, et al., 2002). Our study found FGF2 overexpression in fibrotic tissue and areas of gliosis. Studies in brain tissue of epilepsy patients showed FGF2 overexpression (Sugiura et al., 2008), which increases the excitability and hence susceptibility to seizures, and which also helps to prevent cell death (Zucchini et al., 2008). Therefore, the FGF2 changes demonstrated in this study could promote future studies into the contribution of FGF2 to epileptogenesis in NCC.

In inflammatory processes, angiogenesis is initiated by different cell populations, such as macrophages, mast cells, fibroblasts, and endothelial cells (Granger & Senchenkova, 2010; Imhof & Aurrand-Lions, 2006). These cells produce angiogenic factors such as VEGF, FGF, platelet derived growth factor (PDGF), and tumor necrosis factor alpha (TNF-a), among others. Therefore, it is necessary to establish whether there is an association between the inflammation found in NCC and the expression of the angiogenic markers reported in this study (Lingen, 2001). NCC is a chronic disease and recent studies indicate that angiogenesis accompanied by chronic inflammation tends to intensify and prolong the immune response (Granger & Senchenkova, 2010; Koutroubakis, Tsiolakidou, Karmiris, & Kouroumalis, 2006). Inflammation in NCC could contribute to the production of angiogenic factors, however, in this study, only viable cysts, which tend to have a scarce inflammatory reaction, were evaluated. Our *in vitro* results demonstrated that cysticercus antigens are capable of inducing angiogenesis in the absence of inflammation, leading us to hypothesize that inflammation is not the only cause of angiogenic responses.

We previously reported diffuse IgG staining surrounding cysticerci (M. R. Verastegui et al., 2015). Here we have demonstrated cellular staining, likely representing macrophages or plasma cells. This suggests that IgG diffusion could be a result of the inflammatory response, instead of being caused only BBB leakage. However, our results from endothelial barrier antigen (EBA), reinforce the idea that BBB dysfunction is observed even when cysts are viable. These results are not compatible with previous reports in pigs, where most of viable cysts do not exhibit BBB disruption detected by macroscopic evaluation of Evans blue extravasation (Marzal et al., 2014). Nonetheless, our findings used the IHC staining approach and indicate BBB dysfunction rather than protein extravasation (Pelz et al., 2013).

Even though EBA staining results showed alteration in most of the evaluated cysticerci and Evans blue showed alteration in only a few, it is known that both methods are able to detect different levels of BBB dysfunction (Pelz et al., 2013; Saubaméa, Cochois-Guégan, Cisternino, & Scherrmann, 2012). Evans blue staining demonstrates protein extravasation, whereas EBA is a group of different proteins with an unclear role in BBB maintenance. EBA proteins down regulation has been correlated with BBB dysfunction in different models and diseases. Even though we tested fibrinogen extravasation here, its staining indicates that it is sparsely present in the fibrotic tissue, possibly because there is not enough BBB dysfunction at this level of the disease to allow large proteins such as fibrinogen (340KDa) to move across the BBB and into the brain parenchyma (Wilhelm, Nyúl-Tóth, Suciu, Hermenean, & Krizbai, 2016).

In parenchymal and corticomeningeal cysts, our results demonstrated a greater expression of angiogenic markers (VEGF-A and FGF2) in comparison to the control regions, as well as increases in IgG abundance and number of vessels that are not immunoreactive to EBA. These findings suggest that parenchymal and corticomeningeal cysts have a more intense cellular response compared to ventricular cysts. This may be due to the close contact between the parasite and brain tissue, where cells are more susceptible to tissue injury. The BBB of ventricular cysts was less compromised in comparison to parenchymal and corticomeningeal cysts, possibly due to the fact that ependymal cells protect the subventricular zone as part of the cerebroventricular barrier (Del Bigio, 2010). Additionally, the presence of cerebrospinal fluid could cause parasite antigens to be diluted, which, in turn, could prevent an immune response from being elicited around the ventricles (Lun, Monuki, & Lehtinen, 2015; Xie et al., 2013). Lastly, host-parasite physical contact could mediate injuries in corticomeningeal and parenchymal cysts, but not in ventricular cysts.

Parasites use different pathways to promote their survival and to evade host responses. Helminth antigens have been identified as molecules that promote angiogenesis. For example, beta-thymosin that is present in *Trichinella spiralis* (Kang et al., 2012; Ock & Cha, 2013) and various antigens found in the eggs of *Schistosoma mansoni* have been observed to induce angiogenesis (Kanse et al., 2005). It is hypothesized that helminths can promote angiogenesis via two possible mechanisms: by acting directly in vessels, or, by mediating a proangiogenic response in tissues (Dennis, Schubert, & Bauer, 2011). In this study, novel findings are reported which show that cysticerci can induce tube formation in endothelial cells *in vitro.* This suggests that the cysticercus can directly affect brain vasculature by inducing angiogenesis, as opposed to only activating proangiogenic mechanisms in tissue.

In conclusion, the present study shows that VEGF-A and FGF2 are overexpressed in NCC and that cysticerci antigens can induce angiogenesis. Due to the large roles played by VEGF-A and FGF2 in the processes of cell survival, proliferation, and inflammation, and because of their association with different pathologies of the central nervous system, such as epilepsy, studies of these growth factors could be used to understand the pathology and symptoms found in human NCC.

Supplementary Material

Refer to Web version on PubMed Central for supplementary material.

ACKNOWLEDGEMENTS

The research activities were supported by: National Institutes of Health grant 5D43TW006581 (Infectious Diseases Training Program in Peru) (R.H.G.), National Institutes of Health grant FIC/NIH D43 TW001140, INNOVATE PERU N-135 PNICP-PIAP 2015, CIENCIACTIVA 118–2015-FONDECYT. We would like to thank Cesar Quispe, Francisco Ancajima, Emma Carter, Jemima Morales, Ana Delgado, Gino Castillo, Izabo Guillen and Lizbeth Fustamante as part of the Cysticercosis Working Group in Peru. CONFLICT OF INTEREST

BIBLIOGRAPHY

Alvarez JI, Colegial CH, Castaño CA, Trujillo J, Teale JM, & Restrepo BI (2002). The human nervous tissue in proximity to granulomatous lesions induced by Taenia solium metacestodes displays an active response. Journal of Neuroimmunology, 127(1–2), 139–144. [PubMed: 12044985]

Alvarez JI, Londoño DP, Alvarez AL, Trujillo J, Jaramillo MM, & Restrepo BI (2002). Granuloma formation and parasite disintegration in porcine cysticercosis: comparison with human neurocysticercosis. Journal of Comparative Pathology, 127(2–3), 186–193. [PubMed: 12354530]

Alvarez Jorge I., Mishra BB, Gundra UM, Mishra PK, & Teale JM (2010). Mesocestoides corti intracranial infection as a murine model for neurocysticercosis. Parasitology, 137(03), 359 10.1017/S0031182009991971 [PubMed: 20109250]

Araujo DM, & Cotman CW (1992). Basic FGF in astroglial, microglial, and neuronal cultures: characterization of binding sites and modulation of release by lymphokines and trophic factors. The Journal of Neuroscience: The Official Journal of the Society for Neuroscience, 12(5), 1668–1678. [PubMed: 1578261]

Argaw AT, Asp L, Zhang J, Navrazhina K, Pham T, Mariani JN, … John GR (2012). Astrocyte-derived VEGF-A drives blood-brain barrier disruption in CNS inflammatory disease. Journal of Clinical Investigation, 122(7), 2454–2468. 10.1172/JCI60842 [PubMed: 22653056]

Argaw AT, Gurfein BT, Zhang Y, Zameer A, & John GR (2009). VEGF-mediated disruption of endothelial CLN-5 promotes blood-brain barrier breakdown. Proceedings of the National Academy of Sciences, 106(6), 1977–1982. 10.1073/pnas.0808698106

Argaw AT, Zhang Y, Snyder BJ, Zhao M-L, Kopp N, Lee SC, … John GR (2006). IL-1beta regulates blood-brain barrier permeability via reactivation of the hypoxia-angiogenesis program. Journal of Immunology (Baltimore, Md.: 1950), 177(8), 5574–5584.

Arora N, Tripathi S, Kumar P, Mondal P, Mishra A, & Prasad A (2017). Recent advancements and new perspectives in animal models for Neurocysticercosis immunopathogenesis. Parasite Immunology, 39(7), e12439 10.1111/pim.12439

Baird A, & Walicke PA (1989). Fibroblast growth factors. British Medical Bulletin, 45(2), 438–452. [PubMed: 2480829]

Bar-Klein G, Cacheaux LP, Kamintsky L, Prager O, Weissberg I, Schoknecht K, … Friedman A (2014). Losartan prevents acquired epilepsy via TGF-β signaling suppression: Astrocytic TGF-β and Epilepsy. Annals of Neurology, 75(6), 864–875. 10.1002/ana.24147 [PubMed: 24659129]

Cangalaya C, Zimic M, Marzal M, González AE, Guerra-Giraldez C, Mahanty S, … Cysticercosis Working Group in Peru. (2015). Inflammation Caused by Praziquantel Treatment Depends on the Location of the Taenia solium Cysticercus in Porcine Neurocysticercosis. PLOS Neglected Tropical Diseases, 9(12), e0004207 10.1371/journal.pntd.0004207 [PubMed: 26658257]

Carmeliet P (2003). Angiogenesis in health and disease. Nature Medicine, 9(6), 653–660. 10.1038/nm0603-653

Chandy M, Rajshekhar V, Prakash S, Ghosh S, Joseph T, Abraham J, & Chandi S (1989). CYSTICERCOSIS CAUSING SINGLE, SMALL CT LESIONS IN INDIAN PATIENTS WITH SEIZURES. The Lancet, 333(8634), 390–391. 10.1016/S0140-6736(89)91771-6

de Aluja AS, González D, Rodríguez Carbajal J, & Flisser A (1989). Histological description of tomographic images of Taenia solium cysticerci in pig brains. Clinical Imaging, 13(4), 292–298. [PubMed: 2598111]

Del Bigio MR (2010). Ependymal cells: biology and pathology. Acta Neuropathologica, 119(1), 55–73. 10.1007/s00401-009-0624-y [PubMed: 20024659]

Del Brutto OH (1992). Cysticercosis and cerebrovascular disease: a review. Journal of Neurology, Neurosurgery, and Psychiatry, 55(4), 252–254.

Del Brutto, Oscar H (2012). Diagnostic criteria for neurocysticercosis, revisited. Pathogens and Global Health, 106(5), 299–304. 10.1179/2047773212Y.0000000025 [PubMed: 23265554]

Dennis RD, Schubert U, & Bauer C (2011). Angiogenesis and parasitic helminth-associated neovascularization. Parasitology, 138(04), 426–439. 10.1017/S0031182010001642 [PubMed: 21232174]

Escobar A, Aruffo C, Cruz-Sánchez F, & Cervos-Navarro J (1985). Neuropathologic findings in neurocysticercosis. Archivos De Neurobiologia, 48(3), 151–156. [PubMed: 4062490]

Garcia HH, & Del Brutto OH (2005). Neurocysticercosis: updated concepts about an old disease. The Lancet Neurology, 4(10), 653–661. 10.1016/S1474-4422(05)70194-0 [PubMed: 16168934]

Giavazzi R, Sennino B, Coltrini D, Garofalo A, Dossi R, Ronca R, … Presta M (2003). Distinct Role of Fibroblast Growth Factor-2 and Vascular Endothelial Growth Factor on Tumor Growth and Angiogenesis. The American Journal of Pathology, 162(6), 1913–1926. 10.1016/S0002-9440(10)64325-8 [PubMed: 12759248]

Gómez-Pinilla F, Lee JW, & Cotman CW (1992). Basic FGF in adult rat brain: cellular distribution and response to entorhinal lesion and fimbria-fornix transection. The Journal of Neuroscience: The Official Journal of the Society for Neuroscience, 12(1), 345–355. [PubMed: 1309575]

Gómez-Pinilla F, Vu L, & Cotman CW (1995). Regulation of astrocyte proliferation by FGF-2 and heparan sulfate in vivo. The Journal of Neuroscience: The Official Journal of the Society for Neuroscience, 15(3 Pt 1), 2021–2029. [PubMed: 7891149]

Granger DN, & Senchenkova E (2010). Inflammation and the Microcirculation. San Rafael (CA): Morgan & Claypool Life Sciences Retrieved from http://www.ncbi.nlm.nih.gov/books/NBK53373/

Guerra-Giraldez C, Marzal M, Cangalaya C, Balboa D, Orrego MÁ, Paredes A, … Nash TE (2013). Disruption of the blood–brain barrier in pigs naturally infected with Taenia solium, untreated and after anthelmintic treatment. Experimental Parasitology, 134(4), 443–446. 10.1016/j.exppara.2013.05.005 [PubMed: 23684909]

Imhof BA, & Aurrand-Lions M (2006). Angiogenesis and inflammation face off. Nature Medicine, 12(2), 171–172. 10.1038/nm0206-171

Ivens S, Kaufer D, Flores LP, Bechmann I, Zumsteg D, Tomkins O, … Friedman A (2007). TGF-receptor-mediated albumin uptake into astrocytes is involved in neocortical epileptogenesis. Brain, 130(2), 535–547. 10.1093/brain/awl317 [PubMed: 17121744]

Kang Y-J, Jo J-O, Cho M-K, Yu H-S, Cha H-J, & Ock MS (2012). Trichinella spiralis infection induces β-actin co-localized with thymosin β4. Veterinary Parasitology, 187(3–4), 480–485. 10.1016/j.vetpar.2012.01.017 [PubMed: 22305657]

Kanse SM, Liang O, Schubert U, Haas H, Preissner KT, Doenhoff MJ, & Dennis RD (2005). Characterisation and partial purification of Schistosoma mansoni egg-derived pro-angiogenic factor. Molecular and Biochemical Parasitology, 144(1), 76–85. 10.1016/j.molbiopara.2005.08.001 [PubMed: 16169609]

Koutroubakis IE, Tsiolakidou G, Karmiris K, & Kouroumalis EA (2006). Role of angiogenesis in inflammatory bowel disease. Inflammatory Bowel Diseases, 12(6), 515–523. [PubMed: 16775497]

Lingen MW (2001). Role of leukocytes and endothelial cells in the development of angiogenesis in inflammation and wound healing. Archives of Pathology & Laboratory Medicine, 125(1), 67–71. 10.1043/0003-9985(2001)125<0067:ROLAEC>2.0.CO;2 [PubMed: 11151055]

Liu HM, Yang HB, & Chen RM (1994). Expression of basic fibroblast growth factor, nerve growth factor, platelet-derived growth factor and transforming growth factor-beta in human brain abscess. Acta Neuropathologica, 88(2), 143–150. [PubMed: 7527176]

Lun MP, Monuki ES, & Lehtinen MK (2015). Development and functions of the choroid plexus–cerebrospinal fluid system. Nature Reviews Neuroscience, 16(8), 445–457. 10.1038/nrn3921 [PubMed: 26174708]

Mani N, Khaibullina A, Krum JM, & Rosenstein JM (2005). Astrocyte growth effects of vascular endothelial growth factor (VEGF) application to perinatal neocortical explants: receptor mediation and signal transduction pathways. Experimental Neurology, 192(2), 394–406. 10.1016/j.expneurol.2004.12.022 [PubMed: 15755557]

Marzal M, Guerra-Giraldez C, Paredes A, Cangalaya C, Rivera A, Gonzalez AE, … The Cysticercosis Working Group in Peru. (2014). Evans Blue Staining Reveals Vascular Leakage Associated with Focal Areas of Host-Parasite Interaction in Brains of Pigs Infected with Taenia solium. PLoS ONE, 9(6), e97321 10.1371/journal.pone.0097321 [PubMed: 24915533]

Matos-Silva H, Reciputti BP, Paula E. C. de, Oliveira AL, Moura VBL, Vinaud MC, … Lino-Júnior R. de S. (2012). Experimental encephalitis caused by Taenia crassiceps cysticerci in mice. Arquivos De Neuro-Psiquiatria, 70(4), 287–292. [PubMed: 22358311]

Nash TE, & Garcia HH (2011). Diagnosis and treatment of neurocysticercosis. Nature Reviews Neurology, 7(10), 584–594. 10.1038/nrneurol.2011.135 [PubMed: 21912406]

Ndimubanzi PC, Carabin H, Budke CM, Nguyen H, Qian Y-J, Rainwater E, … Stoner JA (2010). A Systematic Review of the Frequency of Neurocyticercosis with a Focus on People with Epilepsy. PLoS Neglected Tropical Diseases, 4(11), e870 10.1371/journal.pntd.0000870 [PubMed: 21072231]

Obermeier B, Daneman R, & Ransohoff RM (2013). Development, maintenance and disruption of the blood-brain barrier. Nature Medicine, 19(12), 1584–1596. 10.1038/nm.3407

Ock MS, & Cha H-J (2013). Angiogenic Induction by Trichinella spiralis Infection through Thymosin β4. Journal of Life Science, 23(9), 1177–1182. 10.5352/JLS.2013.23.9.1177

Pelz J, Härtig W, Weise C, Hobohm C, Schneider D, Krueger M, … Michalski D (2013). Endothelial barrier antigen-immunoreactivity is conversely associated with blood-brain barrier dysfunction after embolic stroke in rats. European Journal of Histochemistry, 57(4), 38 10.4081/ejh.2013.e38

Renú A, Amaro S, Laredo C, Román LS, Llull L, Lopez A, … Chamorro Á (2015). Relevance of Blood–Brain Barrier Disruption After Endovascular Treatment of Ischemic Stroke: Dual-Energy Computed Tomographic Study. Stroke, 46(3), 673–679. 10.1161/STROKEAHA.114.008147 [PubMed: 25657188]

Restrepo BI, Alvarez JI, Castano JA, Arias LF, Restrepo M, Trujillo J, … Teale JM (2001). Brain Granulomas in Neurocysticercosis Patients Are Associated with a Th1 and Th2 Profile. Infection and Immunity, 69(7), 4554–4560. 10.1128/IAI.69.7.4554-4560.2001 [PubMed: 11401999]

Rigau V, Morin M, Rousset M-C, de Bock F, Lebrun A, Coubes P, … Lerner-Natoli M (2007). Angiogenesis is associated with blood-brain barrier permeability in temporal lobe epilepsy. Brain, 130(7), 1942–1956. 10.1093/brain/awm118 [PubMed: 17533168]

Rosenstein JM, Mani N, Silverman WF, & Krum JM (1998). Patterns of brain angiogenesis after vascular endothelial growth factor administration in vitro and in vivo. Proceedings of the National Academy of Sciences of the United States of America, 95(12), 7086–7091. [PubMed: 9618543]

Ruifrok AC, & Johnston DA (2001). Quantification of histochemical staining by color deconvolution. Analytical and Quantitative Cytology and Histology, 23(4), 291–299. [PubMed: 11531144]

Saubaméa B, Cochois-Guégan V, Cisternino S, & Scherrmann J-M (2012). Heterogeneity in the Rat Brain Vasculature Revealed by Quantitative Confocal Analysis of Endothelial Barrier Antigen and P-Glycoprotein Expression. Journal of Cerebral Blood Flow & Metabolism, 32(1), 81–92. 10.1038/jcbfm.2011.109 [PubMed: 21792241]

Shetty G, Avabratha KS, & Rai BS (2014). Ring-enhancing lesions in the brain: a diagnostic dilemma. Iranian Journal of Child Neurology, 8(3), 61–64. [PubMed: 25143776]

Sikasunge CS, Johansen MV, Phiri IK, Willingham AL, & Leifsson PS (2009). The immune response in Taenia solium neurocysticercosis in pigs is associated with astrogliosis, axonal degeneration and altered blood–brain barrier permeability. Veterinary Parasitology, 160(3–4), 242–250. 10.1016/j.vetpar.2008.11.015 [PubMed: 19117683]

Sköld MK, Gertten CV, Sandbergnordqvist A-C, Mathiesen T, & Holmin S (2005). VEGF and VEGF Receptor Expression after Experimental Brain Contusion in Rat. Journal of Neurotrauma, 22(3), 353–367. 10.1089/neu.2005.22.353 [PubMed: 15785231]

Sugiura C, Miyata H, Ueda M, Ohama E, Vinters HV, & Ohno K (2008). Immunohistochemical expression of fibroblast growth factor (FGF)-2 in epilepsy-associated malformations of cortical development (MCDs). Neuropathology, 28(4), 372–381. 10.1111/j.1440-1789.2007.00881.x [PubMed: 18179408]

Verastegui M, Gilman RH, Arana Y, Barber D, Velasquez J, Farfan M, … and the Cysticercosis Working Group in Peru. (2007). Taenia solium Oncosphere Adhesion to Intestinal Epithelial and Chinese Hamster Ovary Cells In Vitro. Infection and Immunity, 75(11), 5158–5166. 10.1128/IAI.01175-06 [PubMed: 17698575]

Verastegui MR, Mejia A, Clark T, Gavidia CM, Mamani J, Ccopa F, … Gilman RH (2015). Novel Rat Model for Neurocysticercosis Using Taenia solium. The American Journal of Pathology, 185(8), 2259–2268. 10.1016/j.ajpath.2015.04.015 [PubMed: 26216286]

Wilhelm I, Nyúl-Tóth Á, Suciu M, Hermenean A, & Krizbai IA (2016). Heterogeneity of the blood-brain barrier. Tissue Barriers, 4(1), e1143544 10.1080/21688370.2016.1143544 [PubMed: 27141424]

Xie L, Kang H, Xu Q, Chen MJ, Liao Y, Thiyagarajan M, … Nedergaard M (2013). Sleep Drives Metabolite Clearance from the Adult Brain. Science, 342(6156), 373–377. 10.1126/science.1241224 [PubMed: 24136970]

Zucchini S, Buzzi A, Barbieri M, Rodi D, Paradiso B, Binaschi A, … Simonato M (2008). FGF-2 Overexpression Increases Excitability and Seizure Susceptibility but Decreases Seizure-Induced Cell Loss. Journal of Neuroscience, 28(49), 13112–13124. 10.1523/JNEUROSCI.1472-08.2008 [PubMed: 19052202]

MAIN POINTS

Angiogenic factors and BBB disruption are found surrounding T. solium cysticerci.

Cysticerci excretory-secretory products can stimulate angiogenesis.

SIGNIFICANCE

This study is focused on understanding the blood-brain barrier (BBB) alteration which occurs in Neurocysticercosis, the main cause of acquired epilepsy worldwide. We report a novel finding in the T. solium rat model of NCC the overexpression of angiogenic factors and BBB disruption surrounding the cyst. In addition, this study demonstrated that in an endothelial tube formation the parasite products can induce angiogenesis *in vitro*. These results show the effect of the cyst on alteration of the blood-brain barrier.

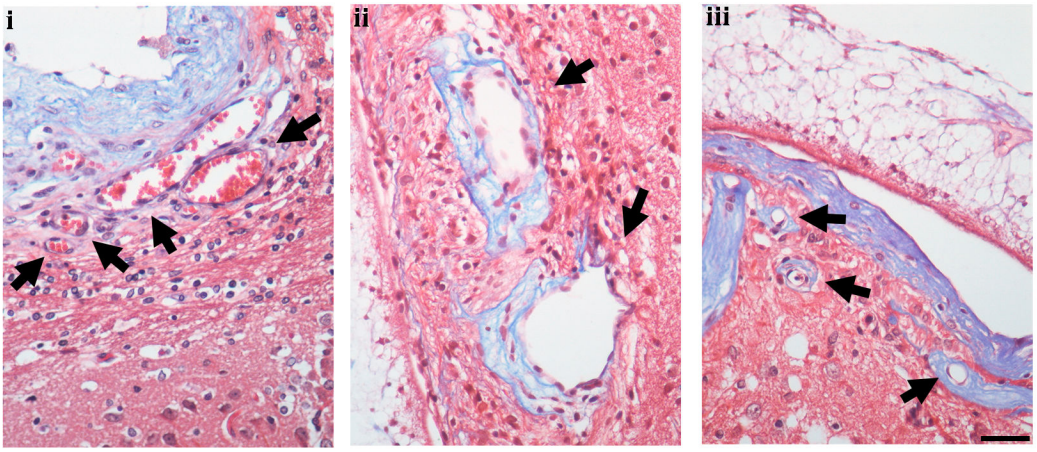

Fig. 1.

Vessel alteration. **i**, dilated vessels without fibrotic tissue (arrow), **ii**, dilated vessels with fibrotic tissue (arrow) and **iii**, sclerotic vessels (arrow) shown by Trichrome Masson staining. Scale bar 50um

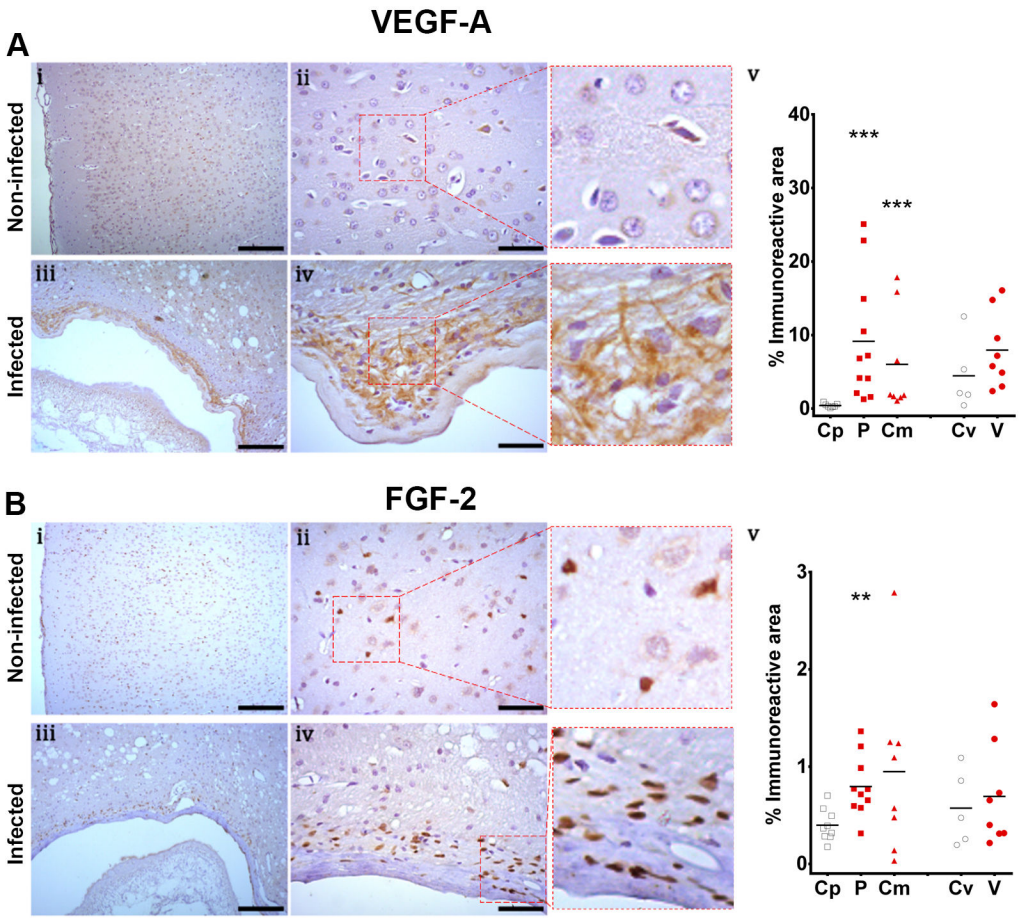

Fig. 2.

Expression of angiogenic factors in NCC model shown by inmunohistochemistry. **Panel A**, VEGF expression, Control region (Cp, [n=7]), parenchymal cyst (P, [n=11]), corticomeningeal cyst (Cm, [n=8]), control region of the ventricle (Cv, [n=5]), ventricular cyst (V, [n=8]). **Panel B**, FGF2 expression. Control region (Cp, [n=9]), parenchymal cyst (P, [n=10]), corticomeningeal cyst (Cm, [n=8]), control region of the ventricle (Cv, [n=5]), ventricular cyst (V, [n=8]). Control brains (**i, ii**) and infected brains (**iii, iv**). **i, iii**, scale bar 200um. **ii, iv**, scale bar 50um. **v**, comparison of the immunoreactive area by cyst location. Mann-Whitney U, P<0.05 (*), P<0.001 (**), P<0.0001 (***)

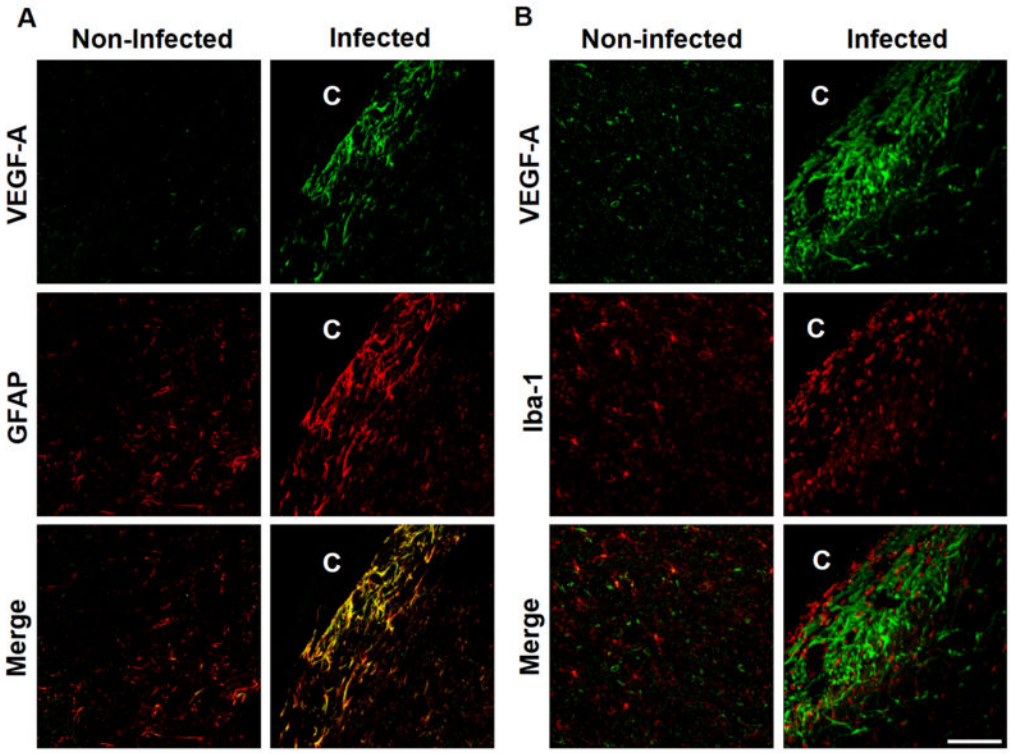

Fig. 3.

VEGF-A and glial cells double staining. C shows cysticercus location. **Panel A,** GFAP and VEGF-A double labeling. Control regions show colocalization between VEGF-A and GFAP and some Iba-1 positive cells colocalize with VEGF-A. Infected regions show most VEGF-A overexpression colocalizing with GFAP. **Panel B**, Iba-1 and VEGF-A double labeling. In control regions some microglial cells colocalized with VEGF-A (yellow). Non-colocalization is observed between Iba-1 and VEGF-A in infected brains. Scale bar 100μm

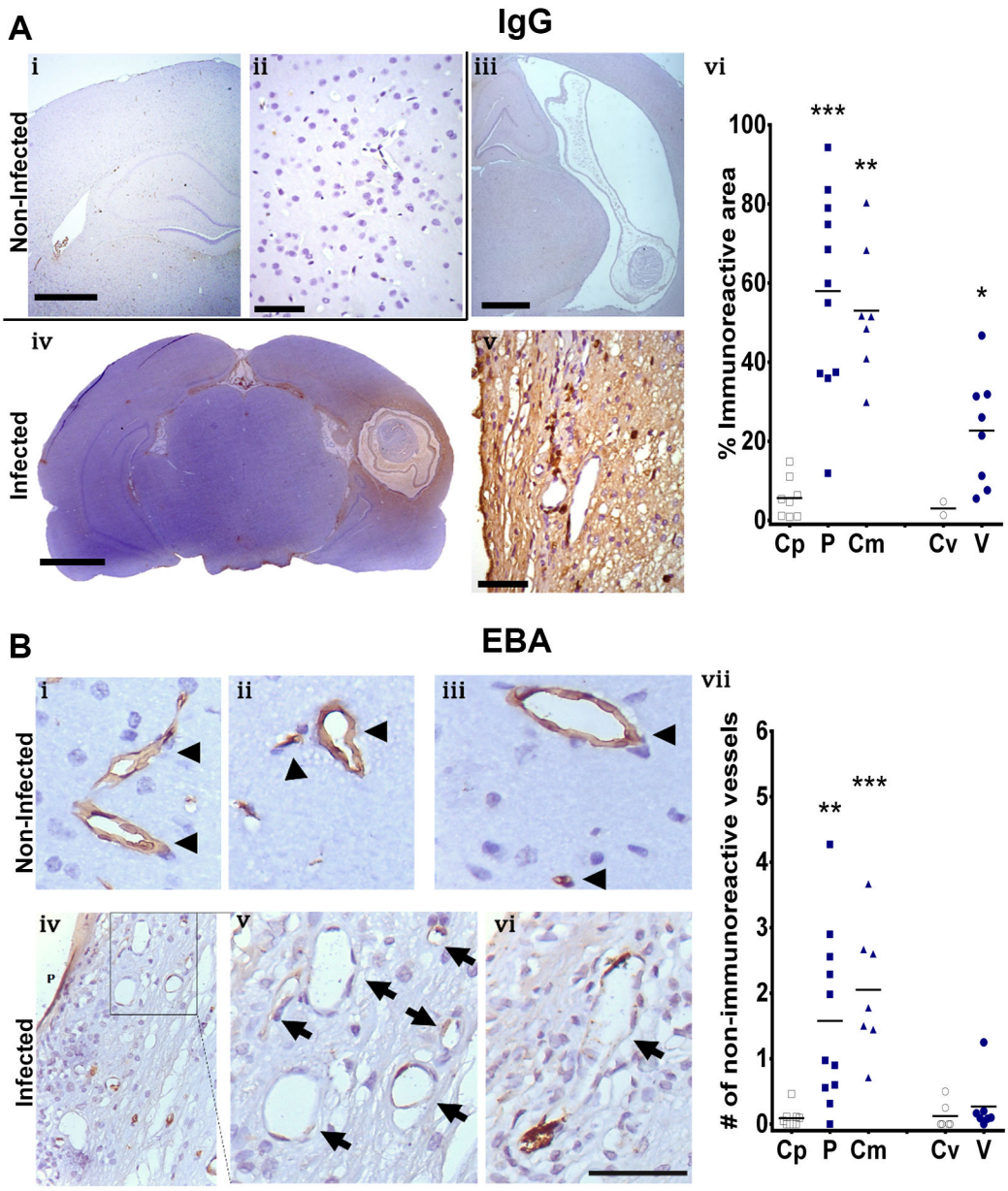

Fig. 4.

IgG and EBA staining for BBB disruption evaluation. **Panel A**, IgG IHC staining. **i** and **ii** represent control brains, reflecting no staining at low (**i**) and high magnification (**ii**). **iii, iv and v** represent infected brains, reflecting ventricular cysts with scarce staining (**iii**), parenchymal cysts with diffuse staining surrounding the cysts (**iv**) and a high magnification image showing some stained cells (**v**). **vi** represents a comparison of the immunoreactive area for IgG staining by cyst location, Control region (Cp, [n=8]), parenchymal cyst (P, [n=11]), corticomeningeal cyst (Cm, [n=7]), control region of the ventricle (Cv, [n=2]), ventricular cyst (V, n=[8]). **i, iii, iv** (scale bar 1mm)**; ii, v**, (scale bar 50μm). **Panel B**, EBA staining. **i, ii** and **iii** represent control brains with normal immunoreactive vessels

(arrowhead)**. iv, v** and **vi** represent infected brains. **vii** represents the comparison of the number of non-immunoreactive vessels per field by cyst location. Control region (Cp, [n=9]), parenchymal cyst (P, [n=11]), corticomeningeal cyst (Cm, [n=7]), control region of the ventricle (Cv, [n=6]), ventricular cyst (V, [n=7]). Mann-Whitney U, $P<0.05$ (*), $P<0.001$ (**), $P<0.0001$ (***)

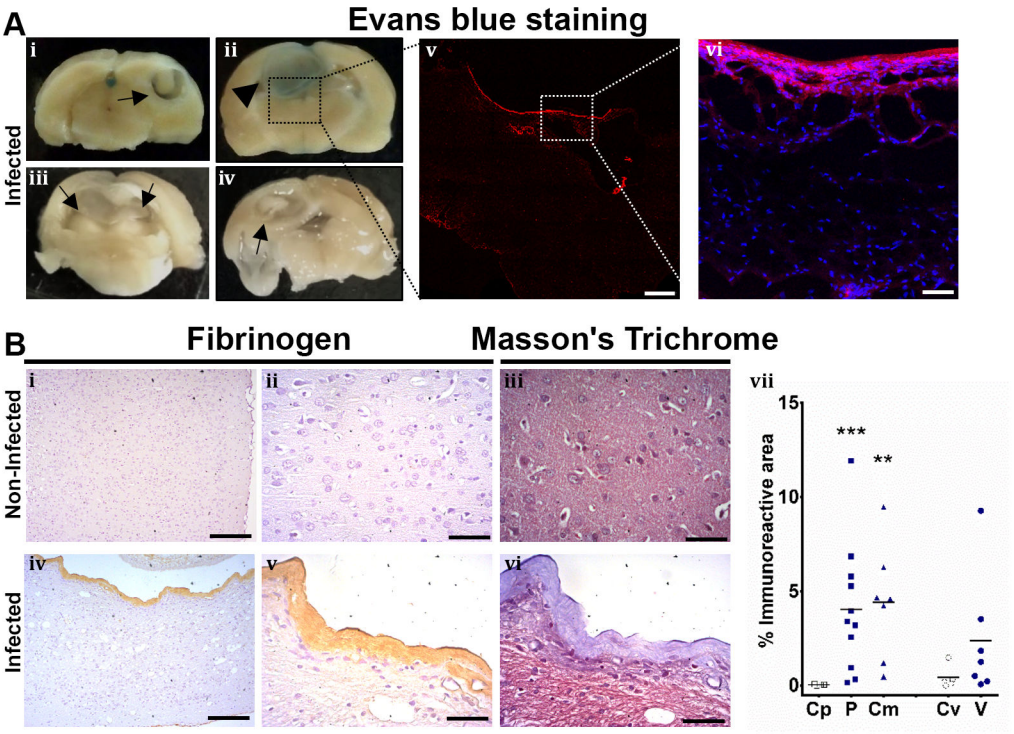

Fig. 5.

Evans blue extravasation and fibrinogen. **Panel A**, Evans blue staining. **i-iv** show the brain of 4 infected rats, arrows show cysts, arrowhead shows blue staining surrounding the cyst. **v**, magnification of iii, shows red fluorescence in the border of the cyst (scale bar, 1mm). **vi**, magnification image shows Evans blue extravasation in the parenchymal tissue (evans blue in red, DAPI in blue, scale bar 50μm). **Panel B**, Fibrinogen presented in fibrosis. **i-iii** represent non-infected brain, no evidence of fibrogen or fibrosis is observed**. iv-vi** shows infected brain, fibrinogen is observed in the fibrotic tissue, confirmed by Masson's trichrome staining. Images at low magnification i and iv, scale bar 200μm. High magnification images, scale bar 50μm. **vii**, shows fibrinogen inmunoreactive area by different cyst location. Control region (Cp, [n=6]), parenchymal cyst (P, [n=11]), corticomeningeal cyst (Cm, [n=7]), control region of the ventricle (Cv, [n=5]), ventricular cyst (V, [n=7]). Mann-Whitney U, $P<0.05$ (*), $P<0.001$ (**), $P<0.0001$ (***)

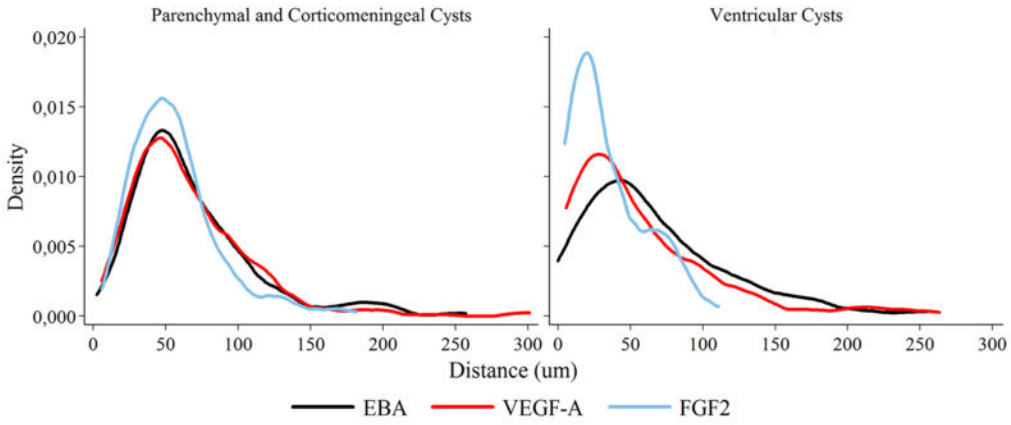

Fig. 6.

Gradient distribution of angiogenic and BBB disruption markers surrounding *T. solium* cysticerci. Distance represents the extension, starting from the border of the tissue in contact with the cyst. In parenchymal and corticomeningeal cysts all markers are similarly codistributed, while in ventricular cysts markers differ in distribution and extension. In both cases, VEGF-A and EBA extend up to approximately 300μm (gliotic area)

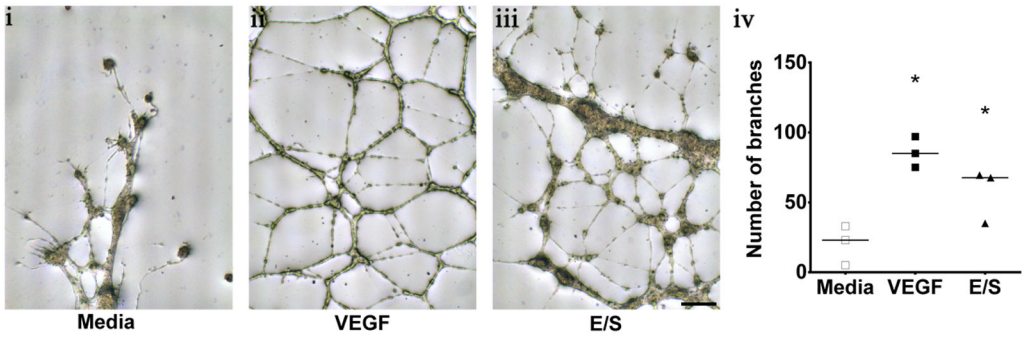

Fig. 7.

Endothelial Cell Tube Formation Assay using HUVEC cell lines. Shows the stimulation of different treatments. **i**, basal media. **ii**, VEGF positive control. **iii**, Cysticercus excretory-secretory antigens (E/S antigens). Scale bar 250μm. **iv**, quantification of the number of branches showing statistically significant difference (*) compared to basal media (Mann-Whitney U test, $P<0.05$, $n=3$ for each group)